



Published in final edited form as:

J Biol Rhythms. 2011 October ; 26(5): 412–422. doi:10.1177/0748730411414170.

Cardiac-Specific Mutation of *Clock* Alters the Quantitative Measurements of Physical Activities without Changing Behavioral Circadian Rhythms

Michael L. Ko^{*}, Liheng Shi^{*}, Ju-Yun Tsai[†], Martin E. Young[‡], Nichole Neuendorff[§], David J. Earnest[§], and Gladys Y.-P. Ko^{*,1}

^{*}Department of Veterinary Integrative Biosciences, College of Veterinary Medicine and Biomedical Sciences, Texas A&M University, College Station, TX

[†]US Department of Agriculture/Agricultural Research Service Children's Nutrition Research Center, Department of Pediatrics, Baylor College of Medicine, Houston, TX

[‡]Division of Cardiovascular Diseases, Department of Medicine, University of Alabama at Birmingham, Birmingham, AL

[§]Department of Neuroscience and Experimental Therapeutics, Texas A&M Health Science Center, College Station, TX

Abstract

Even though peripheral circadian oscillators in the cardiovascular system are known to exist, the daily rhythms of the cardiovascular system are mainly attributed to autonomic or hormonal inputs under the control of the central oscillator, the suprachiasmatic nucleus (SCN). In order to examine the role of peripheral oscillators in the cardiovascular system, we used a transgenic mouse where the *Clock* gene is specifically disrupted in cardiomyocytes. In this cardiomyocyte-specific CLOCK mutant (CCM) mouse model, the circadian input from the SCN remains intact. Both CCM and wild-type (WT) littermates displayed circadian rhythms in wheel-running behavior. However, the overall wheel-running activities were significantly lower in CCM mice compared to WT over the course of 5 weeks, indicating that CCM mice either have lower baseline physical activities or they have lower physical adaptation abilities because daily wheel running, like routine exercise, induces physical adaptation over a period of time. Upon further biochemical analysis, it was revealed that the diurnal oscillations of phosphorylation states of several kinases and protein expression of the L-type voltage-gated calcium channel (L-VGCC) $\alpha 1D$ subunit found in WT hearts were abolished in CCM hearts, indicating that in mammalian hearts, the daily oscillations of the activities of these kinases and L-VGCCs were downstream elements of the cardiac core oscillators. However, the phosphorylation of p38 MAPK exhibited robust diurnal rhythms in both WT and CCM hearts, indicating that cardiac p38 could be under the influence of the central clock through neurohormonal signals or be part of the circadian input pathway in cardiomyocytes. Taken together, these results indicate that the cardiac core oscillators have an impact in regulating circadian rhythmicities and cardiac function.

© 2011 The Author(s)

¹To whom all correspondence should be addressed: Gladys Y.-P. Ko, Department of Veterinary Integrative Biosciences, College of Veterinary Medicine and Biomedical Sciences, Texas A&M University, 4458 TAMU, College Station, TX 77843-4458; gko@cvm.tamu.edu..

CONFLICT OF INTEREST STATEMENT

The author(s) have no potential conflicts of interest with respect to the research, authorship, and/or publication of this article.

Keywords

cardiomyocyte; *Clock*; wheel-running; L-type voltage-gated calcium channel; signaling

The cardiovascular system is known to be under circadian control, and traditionally, its daily rhythms are attributed to autonomic or hormonal inputs governed by the SCN (Yamashita et al., 2003). Nonetheless, circadian changes in the heart from gene expression to metabolism to contractile function are intrinsic and independent of autonomic inputs (Bray et al., 2008; Durgan et al., 2005; Durgan et al., 2006; Young and Bray, 2007). We previously showed that at the cellular level, the L-type voltage-gated calcium channels (L-VGCCs) and phosphorylation states of several signaling molecules, such as extracellular signal-regulated kinase (ERK) and phosphoinositide 3-kinase (PI3K)-protein kinase B (AKT), are under circadian control in chick cardiomyocytes (Ko et al., 2010). However, we obtained heart tissue and cardiomyocytes from entrained whole chicken embryos, making it difficult to dissect the significance of peripheral cardiac oscillators on daily rhythms independent of the master clock. Therefore, we set forth to examine the circadian profiles of cardiomyocyte-specific CLOCK mutant (CCM) mice. In these mice, a dominant-negative mutation of the oscillator gene *Clock* (truncated at the corresponding sequence to the first 541 amino acids) is restricted to cardiomyocytes. This particular animal model offers an exceptional opportunity to isolate circadian input components (from the SCN to the heart through neural/hormonal factors) from the intrinsic oscillators in the heart. The CCM mice allowed us to ascertain local circadian oscillator impact on normal and pathological states of the heart, without affecting the SCN clock and other peripheral oscillators (Bray et al., 2008; Durgan et al., 2005; Durgan and Young, 2010). As such, CCM mice provide advantages that whole animal *Clock* mutant/knockout mice cannot (Vitaterna et al., 2006).

In addition, using CCM mice is in contrast to the study using a transgenic model with brain tissue-specific disruption of the circadian oscillator (Hong et al., 2007). In the transgenic mice with brain tissue-specific disruption of *Clock*, the master clock in the SCN is conditionally altered, and the circadian period of the whole animal is changed (Hong et al., 2007). Because the cardiovascular system is under the control of the autonomic nervous system, in which its circadian rhythm is driven by the SCN, it is possible that the peripheral oscillators in the cardiovascular system are also affected in the transgenic mice with brain tissue-specific disruption of *Clock*. In CCM mice, the circadian circuitry of the body remains intact. The retina is able to transmit light information to the SCN and thereby entrain the SCN. The SCN, in turn, is able to send autonomic or hormonal signals throughout the body including the heart. Therefore, for CCM mice housed under normal light-dark (LD) conditions, elements in the circadian input pathway prior to the core oscillator genes in cardiomyocytes should remain rhythmic. CCM mice display normal daily oscillations as their wild-type (WT) littermates in continuously radiotelemetric-monitored physical activities (such as grooming, sleeping, eating, and moving inside the cage), systolic and diastolic blood pressures, and mean arterial pressure (Bray and Young, 2008). This evidence demonstrates that the circadian input from the SCN to the heart through autonomic means remains intact in CCM mice. However, as a result of the *Clock* mutation in cardiomyocytes, circadian rhythms for elements downstream of the cardiac core oscillators would be either dampened or no longer rhythmic (Bray et al., 2008). Genes encoding enzymes that are responsible for fatty acid metabolism no longer oscillate, and insulin-mediated AKT phosphorylation is decreased in the hearts of CCM mice (Durgan et al., 2010). While the daily oscillation of heart rates in CCM mice is similar to that of the WT mice, CCM mice display bradycardia throughout the entire day (Bray et al., 2008).

Even though there is no apparent pathological problem in CCM mice, as shown in the ultrastructure of CCM cardiomyocytes (Bray et al., 2008), certain changes in the cardiac circadian profiles of CCM mice might have further downstream effects. While wheel-running activity can be used as an indicator of circadian-governed locomotor activity, it also requires higher physical strength and adaptation in contrast to general locomotor activities such as grooming, food intake, or walking. In the present study, we investigated the circadian-driven wheel-running activities of CCM mice and their WT littermates over a 5-week period. We further analyzed the differences in the phosphorylation profiles of several signaling molecules including p42/44 ERK (pERK), p38 MAPK (stress-activated protein kinase), AKT at thr308 (pAKT_{thr308}), and glycogen synthase kinase-3 β (pGSK), as well as the protein expression of the L-type voltage-gated calcium channel α 1D subunit (L-VGCC α 1D) between CCM and WT mice. Our overall results demonstrated that the circadian core oscillator genes in cardiomyocytes play important roles in regulating normal physiological function of the heart, and CCM mice allow us to differentiate between circadian input and output pathways.

MATERIALS AND METHODS

Both WT and CCM male mice (FVB background) were originally generated at the Children's Nutrition Research Facility, Children's Nutrition Research Center, Baylor College of Medicine (Houston, TX). All animal experiments were approved by the Institutional Animal Care and Use Committee of Baylor College of Medicine. All mice were housed under temperature- and humidity-controlled conditions with 12:12-hour LD cycles strictly enforced and fed standard laboratory chow and water ad libitum. Some mice were transferred to Texas A&M University for wheel-running locomotor activity assessment and other experiments.

Wheel-Running Locomotor Activity

All mice between 20 to 28 weeks old were housed individually in cages equipped with running wheels in the animal facility at the Texas A&M University Health Science Center. The procedure used for the wheel-running activity study was approved by the University Laboratory Animal Care Committee at Texas A&M University. All mice were fed standard laboratory chow and water ad libitum. Mice were entrained to 12:12 LD cycles for 5 weeks and then kept in constant darkness (DD; to allow for free-running circadian rhythms) for another 3 weeks. Wheel-running activities were continuously recorded and stored in 10-minute bins, and data were collected and analyzed using ClockLab software (ActiMetrics, Evanston, IL) (Allen et al., 2005). The phase angle of entrainment (Ψ) was assessed under LD conditions. During entrainment, the onset of activity for a given cycle was identified as the first bin during which an animal attained 10% of peak running-wheel revolutions. To measure Ψ , least-squares analysis was used to establish a regression line through the daily onsets of activity during the period of LD entrainment, and then the number of minutes before (positive) or after (negative) the time of lights-off in the LD cycles was determined for each animal. For each animal, the steady-state circadian period (τ) of the activity rhythm in DD was determined by χ^2 periodogram and fast Fourier transform. The total activity count was calculated by averaging the number of wheel revolutions per 24 hours over the 5-week interval of analysis. An activity bout was defined as a period during which wheel-running activity never dropped below 10 counts/bin for more than 20 minutes. These criteria for bout threshold and maximum intrabout interval were used to determine the number of activity bouts per day as well as bout duration (length) and size (average counts per bout). Comparisons between CCM and WT mice were made using the Student t test. Throughout, $p < 0.05$ was regarded as significant.

Preparation of Mouse Heart Samples

Mouse heart samples were collected at both Baylor College of Medicine as well as Texas A&M University. Heart ventricles were isolated from 22-week-old animals at ZT 0, 6, 12, and 18. Heart tissues were subsequently freeze powdered and stored at -80°C . Ventricular RNA was isolated from powdered ventricular tissue using a standard method (Chomczynski and Sacchi, 1987) with Total RNA Isolation Reagent (Molecular Research Center Inc., Cincinnati, OH) and used for quantitative real-time reverse transcription polymerase chain reaction (Q-PCR) assays. Ventricular protein was isolated from powdered ventricular tissue using a standard method with slight modifications (Gibala et al., 2000). Briefly, protein extraction buffer (50 mM Tris-HCl, 150 mM NaCl, 2 mM EGTA, 2 mM EDTA, 2 mM NaF, 2 mM NaPPi, 1% Nonidet P40, 1% glycerol, 5% SDS, 10 mM Na_3VO_4 , 1 mM PMSF, 6.4 μM benzamidine, 0.15 μM aprotinin, 1 μM leupeptin, and 0.73 μM pepstatin A) was added to frozen ventricular powder (25 mg tissue/mL buffer) and immediately homogenized. The homogenates were subsequently centrifuged at 15,000g at 4°C for 15 minutes, and the supernatants were transferred and stored at -80°C prior to assay for protein concentration using the Bradford assay. All samples were diluted to 2 mg/mL and stored for immunoblot analysis.

Immunoblot Analysis

Samples were separated on 10% SDS-PAGE gels and transferred to nitrocellulose membranes as described previously (Ko et al., 2009a; Ko et al., 2007; Ko et al., 2010). The primary antibodies used in this study were anti-VGCC α 1C (Alomone, Jerusalem, Israel), anti-VGCC α 1D (Alomone), anti-phospho308 AKT (pAKT_{thr308}, Cell Signaling Technology, Danvers, MA), anti-phosphoGSK-3 β at ser9 (pGSK, Cell Signaling Technology), anti-phospho stress-activated protein kinase p38 (p38, Cell Signaling Technology), a monoclonal antibody specific for diphospho extracellular signal-related kinase (pERK, Sigma, St. Louis, MO), and a polyclonal antibody insensitive to the phosphorylation state of ERK (total ERK, used for internal and loading control) (Santa Cruz Biochemicals, Santa Cruz, CA). Blots were visualized using appropriate secondary antibodies conjugated to horseradish peroxidase (Cell Signaling Technology) and an ECL detection system (Pierce, Rockford, IL). Relative protein expressions for all proteins involved in this study are reported as a ratio to total ERK because total ERK remains constant throughout the day. The ratio of pERK to total ERK, p38 to total ERK, pAKT to total ERK, pGSK to total ERK, and VGCC to total ERK was determined by densitometry using Scion Image (NIH, Bethesda, MD). For each set of experiments, either the first time point or lowest ratio value of the WT was arbitrarily set to 1. All measurements were repeated at least 3 times.

Quantitative Real-Time RT-PCR

The method used for Q-PCR analysis was described previously (Ko et al., 2007; Ko et al., 2010). Mouse ventricles collected at 4 different time points for Q-PCR were described above. There was 300 ng of total RNA used to quantify the mRNAs of *VGCC α 1C*, *VGCC α 1D*, *Bmal1*, and β -*actin* (loading control) by Q-PCR using the Taqman one-step RT-PCR kit and an ABI Prism 7500 sequence detection system (Applied Biosystems, Foster City, CA). The forward and reverse primers for *Bmal1* were 5'CCAACCCATACACAGAAGCAAAC3' and 5'CTCGGTCACATCCTACGACAAA3'. The forward and reverse primers for *Cacna1c* (the VGCC α 1C subunit) were 5'GGTGAAGCTGCTGAGCCG3' and 5'CAAAGAGCCACATAGGGCAGA3'; the *Cacna1c* probe sequence was 5'FAM-TGGAAGGACTTGATGAAGGTC-QFR3'. The forward and reverse primers for *Cacna1d* (the VGCC α 1D subunit) were 5'GATGGGAATGGCCATGGG3' and 5'GCTTTAGCCTTCTCTTTTCTTGG3'; the *Cacna1d* probe sequence was 5'FAM-ATCATCCTTGGCTCATTTTTTC-QFR3'. All

measurements were repeated at least 3 times. For each individual experiment, a standard curve was generated with known quantities of β -actin mRNA loaded in curved quantities (e.g., 0.5, 1, 2, 4, 8, 16x). The cycle values corresponding to the log values of the curved quantities were used to generate a linear regression formula. The cycle values from the sample RNAs were fit into the formula, and the mRNA quantities of the samples were obtained. The mRNA values of *VGCC α 1C*, *VGCC α 1D*, and *Bmal1* were then divided by the value of β -actin mRNA (loading control), and for each set of experiments, the final mRNA value at the trough was arbitrarily set at 1.

All data are presented as mean \pm SEM (standard error of the mean). One-way ANOVA followed by the Tukey post hoc test for unbalanced n was used for statistical analyses of biochemical and molecular biological assays. Throughout, $p < 0.05$ was regarded as significant. Any defined rhythmic expression at mRNA, protein, or phosphorylation levels had to exhibit at least a 1.5-fold change in rhythmic amplitudes (Karaganis et al., 2008).

RESULTS

Disruption of Cardiac *Clock* Did Not Affect the Circadian Rhythm of Wheel-Running Behavior but Hampered Physical Endurance

Wheel running is a circadian event in mice. It demands higher cardiac workload than routine activities such as grooming, foraging, and walking. Because there is no difference in the circadian rhythms of regular physical activities detected by radiotelemetric infrared beam counts between CCM mice and their WT littermates (Bray et al., 2008), we set forth to examine whether interruption of *Clock* in the heart would have any impact on circadian wheel-running behavior rhythms in CCM mice.

WT (Fig. 1A) and CCM mice (Fig. 1B) double-plotted actograms in LD (A1, B1) and DD (A2, B2) show no statistical difference in phase angle of entrainment (Ψ ; WT = 2.06 ± 0.89 hours, CCM = 1.67 ± 0.88 hours) or steady-state circadian period (τ ; WT = 23.52 ± 0.06 hours, CCM = 23.96 ± 0.28 hours; WT: $n = 21$, CCM: $n = 17$). However, there was a difference in the quantitative parameters of wheel-running behavior. The WT mice had significantly higher numbers of total wheel revolutions per day (total activity counts) (Fig. 1C). Upon further analysis, we found that even though there was no difference in the total bouts per day between WT and CCM mice (Fig. 1D), CCM mice had shorter bout durations (34% less) (Fig. 1E). The average counts of wheel revolutions per bout were also significantly lower in CCM mice, in which there was a 44% decrease compared to the WT (Fig. 1F). In addition, the overall daily average of activity counts in CCM mice is 30% less than the WT (Fig. 1C). These results show that cardiomyocyte-specific *Clock* disruption did not alter circadian entrainment or free-running period in CCM mice but affected cardiac-related exercise capabilities, as presumably reflected by the aforementioned reductions in total activity and other quantitative parameters of wheel-running behavior. The CCM mice used in this study (FVB genetic background) (Bray et al., 2008; Taketo et al., 1991) took longer (~7-10 days) to entrain to wheel-running activities in LD (as shown in the initial days of the actograms) compared to other mouse strains such as C57BL/6J. This delay could be due to other reasons such as recognition of the wheel at the visual or cognitive level but not strictly to circadian entrainment.

The Phosphorylation States of Several Signaling Molecules Were under Cardiac Circadian Control

Because CCM mice had significantly lower wheel-running activities than the WT in the quantitative analysis, we next examined whether the circadian rhythms of the phosphorylation states of several signaling molecules important in many cardiac

physiological conditions and function, including ERK, p38, AKT, and GSK-3 β , were altered in CCM mouse hearts. Both ERK and p38 have been implicated in regulating cardiac contractility and the development of various pathological states such as cardiac hypertrophy and heart failure because they control cell growth and proliferation (Olson and Molkenin, 1999; Sugden, 1999; Szokodi et al., 2008). Also, in human failing hearts, the activity of GSK-3 β is greatly inhibited (Haq et al., 2001). The phosphorylation states of ERK (diphosphorylated; pERK) and p38 (phosphorylated p38; p38) displayed diurnal rhythms in WT ventricles (Fig. 2A and 2B). While pERK peaked at ZT 0 (Fig. 2A), p38 peaked at ZT 12 (Fig. 2B). Interestingly, in CCM mice, pERK was no longer rhythmic (Fig. 2A), while p38 remained rhythmic (Fig. 2B). In WT mice, phosphorylation of AKT at thr308 (pAKT_{thr308}) peaked at ZT 6 (Fig. 2C), while the phosphorylation of its downstream target GSK-3 β (pGSK) peaked at ZT 12 to 18 (~6-hour lag behind pAKT_{thr308}) (Fig. 2D). In CCM mouse ventricles, both pAKT_{thr308} (Fig. 2C) and pGSK (Fig. 2D) were no longer rhythmic. Hence, the phosphorylation states of ERK, AKT_{thr308}, and GSK were under cardiac *Clock* gene control in the ventricles, while the p38 rhythm was driven by other circadian inputs, possibly from the SCN, to the heart.

Disruption of *Clock* in the Heart Dampened the Daily Oscillations of Ventricular *Bmal1* and Abolishes Those for VGCC α 1D

While heart rates of CCM and WT mice have similar circadian oscillation patterns, overall heart rates of CCM mice are slower than the WT throughout the entire day (Bray et al., 2008). The L-type voltage-gated calcium channel (L-VGCC) consists of a pore-forming α_1 subunit and regulatory β and $\alpha_2\delta$ subunits (Takahashi et al., 1987; Wang et al., 2004). Among major L-VGCC α 1 subunits, VGCC α 1C (CaV1.2) and α 1D (CaV1.3) are the most prevalent in the heart and play important roles in cardiac physiology. In both humans and mice, the α 1D subunit is expressed in both ventricles and atria but at lower quantities compared to the α 1C subunit (Gaborit et al., 2007; Zhang et al., 2005).

Previously, we showed that in chick embryonic hearts, the mRNA and protein levels of both VGCC α 1C and α 1D are under circadian control (Ko et al., 2010). However, in rats, there is no diurnal rhythm of VGCC α 1C protein expression, even though the L-VGCC current density recorded from ventricular cardiomyocytes is rhythmic (Collins and Rodrigo, 2010). Hence, we set forth to investigate whether VGCC α 1 subunits were rhythmic in mouse hearts. The mRNA levels and protein expression of VGCC α 1C remained constant throughout the day in both WT and CCM mouse ventricles (Fig. 3A and 3B), while the mRNA levels and protein expression of VGCC α 1D displayed daily rhythms in WT mice (Fig. 3C and 3D). The protein expression of VGCC α 1D peaked at ZT 6, with an approximately 6-hour delay from the peak mRNA level in WT mice (Fig. 3D). The daily rhythms in VGCC α 1D mRNA and protein levels were abolished in CCM mice (Fig. 3C and 3D). In addition, *Bmal1* mRNA remained rhythmic in CCM mice but at a lower oscillation amplitude compared to the WT (Fig. 3E). The diurnal patterns of *Bmal1* in both WT and CCM mice matched those previously published (see Suppl. Fig. S5 of Bray et al. [2008]). Therefore, interruption of the cardiac circadian oscillator abolished the diurnal rhythms of L-VGCC α 1D.

DISCUSSION

There are intrinsic circadian changes in cardiac metabolism (Bray et al., 2008; Durgan and Young, 2010; Young et al., 2001), contractile function (Young et al., 2001), and expression of circadian clock genes (Storch et al., 2002; Young, 2003; Young et al., 2001) that are independent of autonomic inputs. Cardiomyocyte responses to starvation or fatty acid overload are also under the control of intrinsic circadian oscillators (Durgan et al., 2006; Stavinoha et al., 2004; Young et al., 2001). Disruption of cardiac circadian oscillators alters

cardiac response to insults (Durgan et al., 2010; Virag et al., 2010). Therefore, the intrinsic clocks in cardiomyocytes play critical roles in preparing the heart to anticipate daily workload and synchronizing cardiac metabolism and responses to the environment (Durgan et al., 2005; Young, 2006).

There is no difference between WT and CCM mice in quantitative measurements of daily rhythms in routine activities (such as foraging, grooming, sleeping, and walking) using radiotelemetric infrared beam detection (Bray et al., 2008), and the diurnal rhythms of wheel-running activities were also similar between CCM and WT mice (Fig. 1A). These observations demonstrate that the light information from the retina to the SCN and the subsequent circadian entrainment input from the SCN are intact in CCM mice. However, we observed that CCM mice displayed less overall quantitative physical activity. The mice used in the behavior study were 20 to 28 weeks old, with no difference in body weight between WT and CCM mice (data not shown). Thus, neither age nor obesity was a contributing factor to the decrease in physical activity in CCM mice. One possible explanation is that the *Clock* disruption in cardiomyocytes changes the metabolic and physical state of the heart, in which the circadian oscillations of certain molecules (mRNA and protein levels, as well as phosphorylation states of certain proteins) are suspended at the resting state (around ZT 0) (Durgan et al., 2010; Durgan and Young, 2010; Tsai et al., 2010). Daily wheel running resembles regular physical exercise training for a few hours every day, which is more strenuous than ordinary routine physical activities. Therefore, wheel running requires higher physical activity and cardiac workload. If the cardiac condition of CCM mice is suspended at the resting state, it is possible that their baseline physical activity is lower, which leads to lower wheel-running activities. Regular daily exercise also causes physical adaptation in cardiac output and capacity (Duncker and Bache, 2008; Kemi et al., 2008). An alternative explanation is that overall physical adaptation to wheel-running activities in CCM mice is lower than WT mice because our quantitative wheel-running measurements were the results across 5 weeks. Therefore, interruption of the cardiomyocyte-specific oscillator subsequently led to less baseline activity or adaptation to physical exercise as demonstrated by wheel-running activities. This observation also reveals the importance of peripheral oscillators to overall health: even though animals were maintained under LD conditions, the absence of functional circadian oscillators in the heart may have compromised physical activities. In the long term, there could be more detrimental effects and potentially premature aging in these animals compared to their WT littermates, which would be very interesting and worth investigation.

Both ERK and PI3K-AKT signaling pathways are important in physiological and pathological states of cardiomyocytes, and in most cases, these pathways regulate cardiac function independently. However, one potential converging point is through phosphorylation of GSK3 because activation of ERK by endothelin and activation of PI3K-AKT through insulin can both lead to phosphorylation of GSK3 (Gonzalez et al., 2007). Therefore, the phosphorylation state of GSK3 could potentially be affected by either PI3K-AKT or ERK or both. These 2 pathways also play important roles in regulating circadian rhythms in various species and organs. p42/44 ERK, a kinase in the MAPK-Erk family, is particularly involved in the circadian entrainment of the mammalian SCN (Butcher et al., 2002; Obrietan et al., 1998) but serves in the circadian output in the avian retina and pineal gland (Ko et al., 2001; Ko et al., 2009b; Yadav et al., 2003). Another MAP kinase, p38, participates in light-dependent phase shifting in *Xenopus* retinal photoreceptors (Hasegawa and Cahill, 2004) and circadian inputs in mammalian cell lines (Moldrup et al., 2010; Petrzilka et al., 2009; Qu et al., 2008) but serves as a circadian output in *Neurospora* (Vitalini et al., 2007). Although changing AKT activity alters circadian periods in *Drosophila* (Zheng and Sehgal, 2010), the PI3K-AKT pathway is part of the circadian output to regulate Ca²⁺ channel activities in avian retinal photoreceptors (Ko et al., 2009a). Furthermore, GSK3 β , a downstream target of

PI3K-AKT, is known to regulate the circadian period in mammalian clocks through interactions with core oscillator genes (Hirota et al., 2008; Iitaka et al., 2005; Sahar et al., 2010). For example, mammalian GSK-3 β is known to regulate the molecular clock by phosphorylating CRY2 (Kurabayashi et al., 2006), PER2 (Iitaka et al., 2005), and BMAL1 (Sahar et al., 2010). Thus, alterations in GSK-3 β phosphorylation or expression cause changes in circadian phases (Iitaka et al., 2005).

Because the studies of these signaling pathways in circadian inputs/outputs were done in different organs or species, we took advantage of using CCM mice as a tool to access the roles of PI3K-AKT and ERK as circadian input/output pathways. We found that the phosphorylation states of pERK, p38, pAKT_{thr308}, and pGSK were rhythmic in WT mice kept in LD cycles, while they seemed to be suspended at resting period levels in CCM mice kept in LD. The “suspension” of the daily oscillation of these kinase activities correlates to the lower wheel-running activities in CCM mice. Thus, it is possible that the cardiac-specific *Clock* disruption somehow “suspends” physical activity at the resting period level. This theory will require further investigation. Interestingly, the diurnal rhythm of phosphorylated p38 was unchanged in CCM mouse hearts, which indicates that either p38 could be upstream of cardiac core oscillators and part of the circadian input pathway to the mouse heart or p38 is regulated by the daily oscillation of neurohormonal signals to the heart. The other kinases investigated in the present study (ERK, AKT, and GSK) were downstream of cardiac oscillators, and therefore, these kinases could be in the circadian output pathway in mouse cardiomyocytes. Further studies to dissect the elements of circadian input and output pathways in the heart will be needed.

Calcium that enters the cardiomyocyte via L-VGCCs triggers a more substantial Ca²⁺ release from the sarcoplasmic reticulum (Altamirano and Bers, 2007). This Ca²⁺-induced Ca²⁺ release in cardiomyocytes underlies the control of cardiac contraction force during excitation-contraction (E-C) coupling (Altamirano and Bers, 2007; Kranias and Bers, 2007). Therefore, L-VGCCs affect E-C coupling, contractile force, and cardiac output in adult animals (Fauconner et al., 2003; Kubalova, 2003). Previously, Collins and Rodrigo (2010) found that there are diurnal variations in all parameters of E-C coupling as well as L-VGCC currents recorded from rat ventricular cardiomyocytes. However, it is perplexing as to why the L-VGCC current density is higher during the active period, while other E-C coupling parameters including diastolic Ca²⁺, basal systolic Ca²⁺, contraction strength, and cell shortening are higher during the resting period. In chicken embryonic hearts, mRNA and protein levels of L-VGCCs (both α 1C and α 1D) as well as L-VGCC currents are under circadian control, which are higher at night (Ko et al., 2010). Here, we showed that the protein level of L-VGCC α 1D, but not α 1C, was high during the day (resting period) in WT mice, while in CCM mice, the VGCC α 1D protein level remained at a lower constant level throughout the day. We postulate that there could be a species-dependent regulation of the circadian rhythm of L-VGCC α 1 subunits and their potential physiological roles, which will require future studies. Taken together, using CCM mice as an animal model, we were able to dissect the circadian light-sensitive input and output pathways in cardiomyocytes. More importantly, we demonstrated that without functional peripheral oscillators, the organism's health could be under great distress.

Acknowledgments

This work was supported in part by a start-up fund from Texas A&M University and NIH RO1 EY017452 to G.Y.K., NIH PO1 NS39546 to D.J.E., and NIH RO1 HL-074259 to M.E.Y.

REFERENCES

- Allen GC, West JR, Chen WJ, Earnest DJ. Neonatal alcohol exposure permanently disrupts the circadian properties and photic entrainment of the activity rhythm in adult rats. *Alcohol Clin Exp Res.* 2005; 29:1845–1852. [PubMed: 16269914]
- Altamirano J, Bers DM. Voltage dependence of cardiac excitation-contraction coupling: unitary Ca²⁺ current amplitude and open channel probability. *Circ Res.* 2007; 101:590–597. [PubMed: 17641229]
- Bray MS, Shaw CA, Moore MW, Garcia RA, Zanquetta MM, Durgan DJ, Jeong WJ, Tsai JY, Bugger H, Zhang D, et al. Disruption of the circadian clock within the cardiomyocyte influences myocardial contractile function, metabolism, and gene expression. *Am J Physiol Heart Circ Physiol.* 2008; 294:H1036–H1047. [PubMed: 18156197]
- Bray MS, Young ME. Diurnal variations in myocardial metabolism. *Cardiovasc Res.* 2008; 79:228–237. [PubMed: 18304930]
- Butcher GQ, Doner J, Dziema H, Collamore M, Burgoon PW, Obrietan K. The p42/44 mitogen-activated protein kinase pathway couples photic input to circadian clock entrainment. *J Biol Chem.* 2002; 277:29519–29525. [PubMed: 12042309]
- Chomczynski P, Sacchi N. Single-step method of RNA isolation by acid guanidinium thiocyanate-phenol-chloroform extraction. *Anal Biochem.* 1987; 162:156–159. [PubMed: 2440339]
- Collins HE, Rodrigo GC. Inotropic response of cardiac ventricular myocytes to beta-adrenergic stimulation with isoproterenol exhibits diurnal variation: involvement of nitric oxide. *Circ Res.* 2010; 106:1244–1252. [PubMed: 20167926]
- Duncker DJ, Bache RJ. Regulation of coronary blood flow during exercise. *Physiol Rev.* 2008; 88:1009–1086. [PubMed: 18626066]
- Durgan DJ, Hotze MA, Tomlin TM, Egbejimi O, Graveleau C, Abel ED, Shaw CA, Bray MS, Hardin PE, Young ME. The intrinsic circadian clock within the cardiomyocyte. *Am J Physiol Heart Circ Physiol.* 2005; 289:H1530–H1541. [PubMed: 15937094]
- Durgan DJ, Pulinilkunnit T, Villegas-Montoya C, Garvey ME, Frangogiannis NG, Michael LH, Chow CW, Dyck JR, Young ME. Short communication. Ischemia/reperfusion tolerance is time-of-day-dependent: mediation by the cardiomyocyte circadian clock. *Circ Res.* 2010; 106:546–550. [PubMed: 20007913]
- Durgan DJ, Trexler NA, Egbejimi O, McElfresh TA, Suk HY, Petterson LE, Shaw CA, Hardin PE, Bray MS, Chandler MP, et al. The circadian clock within the cardiomyocyte is essential for responsiveness of the heart to fatty acids. *J Biol Chem.* 2006; 281:24254–24269. [PubMed: 16798731]
- Durgan DJ, Young ME. The cardiomyocyte circadian clock: emerging roles in health and disease. *Circ Res.* 2010; 106:647–658. [PubMed: 20203314]
- Fauconnier J, Bedut S, Le Guennec JY, Babuty D, Richard S. Ca²⁺ current-mediated regulation of action potential by pacing rate in rat ventricular myocytes. *Cardiovasc Res.* 2003; 57:670–680. [PubMed: 12618229]
- Gaborit N, Le Bouter S, Szuts V, Varro A, Escande D, Nattel S, Demolombe S. Regional and tissue specific transcript signatures of ion channel genes in the non-diseased human heart. *J Physiol.* 2007; 582:675–693. [PubMed: 17478540]
- Gibala MJ, Young ME, Taegtmeyer H. Anaplerosis of the citric acid cycle: role in energy metabolism of heart and skeletal muscle. *Acta Physiol Scand.* 2000; 168:657–665. [PubMed: 10759602]
- Gonzalez A, Ravassa S, Loperena I, Lopez B, Beaumont J, Querejeta R, Larman M, Diez J. Association of depressed cardiac gp130-mediated antiapoptotic pathways with stimulated cardiomyocyte apoptosis in hypertensive patients with heart failure. *J Hypertens.* 2007; 25:2148–2157. [PubMed: 17885560]
- Haq S, Choukroun G, Lim H, Tymitz KM, del Monte F, Gwathmey J, Grazette L, Michael A, Hajjar R, Force T, Molkenin JD. Differential activation of signal transduction pathways in human hearts with hypertrophy versus advanced heart failure. *Circulation.* 2001; 103:670–677. [PubMed: 11156878]

- Hasegawa M, Cahill GM. Regulation of the circadian oscillator in *Xenopus* retinal photoreceptors by protein kinases sensitive to the stress-activated protein kinase inhibitor, SB 203580. *J Biol Chem.* 2004; 279:22738–22746. [PubMed: 15028715]
- Hirota T, Lewis WG, Liu AC, Lee JW, Schultz PG, Kay SA. A chemical biology approach reveals period shortening of the mammalian circadian clock by specific inhibition of GSK-3 β . *Proc Natl Acad Sci U S A.* 2008; 105:20746–20751. [PubMed: 19104043]
- Hong HK, Chong JL, Song W, Song EJ, Jyawook AA, Schook AC, Ko CH, Takahashi JS. Inducible and reversible Clock gene expression in brain using the tTA system for the study of circadian behavior. *PLoS Genet.* 2007; 3:e33. [PubMed: 17319750]
- Iitaka C, Miyazaki K, Akaike T, Ishida N. A role for glycogen synthase kinase-3 β in the mammalian circadian clock. *J Biol Chem.* 2005; 280:29397–29402. [PubMed: 15972822]
- Karaganis SP, Kumar V, Beremand PD, Bailey MJ, Thomas TL, Cassone VM. Circadian genomics of the chick pineal gland in vitro. *BMC Genomics.* 2008; 9:206. [PubMed: 18454867]
- Kemi OJ, Ellingsen O, Smith GL, Wisloff U. Exercise-induced changes in calcium handling in left ventricular cardiomyocytes. *Front Biosci.* 2008; 13:356–368. [PubMed: 17981553]
- Ko GY, Ko ML, Dryer SE. Circadian regulation of cGMP-gated cationic channels of chick retinal cones: Erk MAP Kinase and Ca²⁺/calmodulin-dependent protein kinase II. *Neuron.* 2001; 29:255–266. [PubMed: 11182096]
- Ko ML, Jian K, Shi L, Ko GY. Phosphatidylinositol 3 kinase-Akt signaling serves as a circadian output in the retina. *J Neurochem.* 2009a; 108:1607–1620. [PubMed: 19166512]
- Ko ML, Liu Y, Dryer SE, Ko GY. The expression of L-type voltage-gated calcium channels in retinal photoreceptors is under circadian control. *J Neurochem.* 2007; 103:784–792. [PubMed: 17683482]
- Ko ML, Shi L, Grushin K, Nigussie F, Ko GY. Circadian profiles in the embryonic chick heart: L-type voltage-gated calcium channels and signaling pathways. *Chronobiol Int.* 2010; 27:1673–1696. [PubMed: 20969517]
- Ko ML, Shi L, Ko GY. Circadian controls outweigh acute illumination effects on the activity of extracellular signal-regulated kinase (ERK) in the retina. *Neurosci Lett.* 2009b; 451:74–78. [PubMed: 19111596]
- Kranias EG, Bers DM. Calcium and cardiomyopathies. *Subcell Biochem.* 2007; 45:523–537. [PubMed: 18193651]
- Kubalova Z. Inactivation of L-type calcium channels in cardiomyocytes: experimental and theoretical approaches. *Gen Physiol Biophys.* 2003; 22:441–454. [PubMed: 15113117]
- Kurabayashi N, Hirota T, Harada Y, Sakai M, Fukada Y. Phosphorylation of mCRY2 at Ser557 in the hypothalamic suprachiasmatic nucleus of the mouse. *Chronobiol Int.* 2006; 23:129–134. [PubMed: 16687286]
- Moldrup ML, Georg B, Falktoft B, Mortensen R, Hansen JL, Fahrenkrug J. Light induces Fos expression via extracellular signal-regulated kinases 1/2 in melanopsin-expressing PC12 cells. *J Neurochem.* 2010; 112:797–806. [PubMed: 19943848]
- Obrietan K, Impey S, Storm DR. Light and circadian rhythmicity regulate MAP kinase activation in the suprachiasmatic nuclei. *Nat Neurosci.* 1998; 1:693–700. [PubMed: 10196585]
- Olson EN, Molkentin JD. Prevention of cardiac hypertrophy by calcineurin inhibition: hope or hype? *Circ Res.* 1999; 84:623–632. [PubMed: 10189350]
- Petrzilka S, Taraborrelli C, Cavadini G, Fontana A, Birchler T. Clock gene modulation by TNF- α depends on calcium and p38 MAP kinase signaling. *J Biol Rhythms.* 2009; 24:283–294. [PubMed: 19625730]
- Qu Y, Mao M, Li X, Liu Y, Ding J, Jiang Z, Wan C, Zhang L, Wang Z, Mu D. Telomerase reconstitution contributes to resetting of circadian rhythm in fibroblasts. *Mol Cell Biochem.* 2008; 313:11–18. [PubMed: 18398672]
- Sahar S, Zocchi L, Kinoshita C, Borrelli E, Sassone-Corsi P. Regulation of BMAL1 protein stability and circadian function by GSK3 β -mediated phosphorylation. *PLoS One.* 2010; 5:e8561. [PubMed: 20049328]
- Stavinoha MA, Rayspellicy JW, Hart-Sailors ML, Mersmann HJ, Bray MS, Young ME. Diurnal variations in the responsiveness of cardiac and skeletal muscle to fatty acids. *Am J Physiol Endocrinol Metab.* 2004; 287:E878–E887. [PubMed: 15292029]

- Storch KF, Lipan O, Leykin I, Viswanathan N, Davis FC, Wong WH, Weitz CJ. Extensive and divergent circadian gene expression in liver and heart. *Nature*. 2002; 417:78–83. [PubMed: 11967526]
- Sugden PH. Signaling in myocardial hypertrophy: life after calcineurin? *Circ Res*. 1999; 84:633–646. [PubMed: 10189351]
- Szokodi I, Kerkela R, Kubin AM, Sarman B, Pikkarainen S, Konyi A, Horvath IG, Papp L, Toth M, Skoumal R, Ruskoaho H. Functionally opposing roles of extracellular signal-regulated kinase 1/2 and p38 mitogen-activated protein kinase in the regulation of cardiac contractility. *Circulation*. 2008; 118:1651–1658. [PubMed: 18824646]
- Takahashi M, Seagar MJ, Jones JF, Reber BF, Catterall WA. Subunit structure of dihydropyridine-sensitive calcium channels from skeletal muscle. *Proc Natl Acad Sci U S A*. 1987; 84:5478–5482. [PubMed: 2440051]
- Taketo M, Schroeder AC, Mobraaten LE, Gunning KB, Hanten G, Fox RR, Roderick TH, Stewart CL, Lilly F, Hansen CT, et al. FVB/N: an inbred mouse strain preferable for transgenic analyses. *Proc Natl Acad Sci U S A*. 1991; 88:2065–2069. [PubMed: 1848692]
- Tsai JY, Kienesberger PC, Pulinilkunnil T, Sailors MH, Durgan DJ, Villegas-Montoya C, Jahoor A, Gonzalez R, Garvey ME, Boland B, et al. Direct regulation of myocardial triglyceride metabolism by the cardiomyocyte circadian clock. *J Biol Chem*. 2010; 285:2918–2929. [PubMed: 19940111]
- Virag JA, Dries JL, Easton PR, Friesland AM, DeAntonio JH, Chintalgattu V, Cozzi E, Lehmann BD, Ding JM, Lust RM. Attenuation of myocardial injury in mice with functional deletion of the circadian rhythm gene *mPer2*. *Am J Physiol Heart Circ Physiol*. 2010; 298:H1088–H1095. [PubMed: 20061537]
- Vitalini MW, de Paula RM, Goldsmith CS, Jones CA, Borkovich KA, Bell-Pedersen D. Circadian rhythmicity mediated by temporal regulation of the activity of p38 MAPK. *Proc Natl Acad Sci U S A*. 2007; 104:18223–18228. [PubMed: 17984065]
- Vitaterna MH, Ko CH, Chang AM, Buhr ED, Fruechte EM, Schook A, Antoch MP, Turek FW, Takahashi JS. The mouse *Clock* mutation reduces circadian pacemaker amplitude and enhances efficacy of resetting stimuli and phase-response curve amplitude. *Proc Natl Acad Sci U S A*. 2006; 103:9327–9332. [PubMed: 16754844]
- Wang MC, Collins RF, Ford RC, Berrow NS, Dolphin AC, Kitmitto A. The three-dimensional structure of the cardiac L-type voltage-gated calcium channel: comparison with the skeletal muscle form reveals a common architectural motif. *J Biol Chem*. 2004; 279:7159–7168. [PubMed: 14634003]
- Yadav G, Straume M, Heath J 3rd, Zatz M. Are changes in MAPK/ERK necessary or sufficient for entrainment in chick pineal cells? *J Neurosci*. 2003; 23:10021–10031. [PubMed: 14602816]
- Yamashita T, Sekiguchi A, Iwasaki YK, Sagara K, Iinuma H, Hatano S, Fu LT, Watanabe H. Circadian variation of cardiac K⁺ channel gene expression. *Circulation*. 2003; 107:1917–1922. [PubMed: 12668525]
- Young ME. Circadian rhythms in cardiac gene expression. *Curr Hypertens Rep*. 2003; 5:445–453. [PubMed: 14594562]
- Young ME. The circadian clock within the heart: potential influence on myocardial gene expression, metabolism, and function. *Am J Physiol Heart Circ Physiol*. 2006; 290:H1–H16. [PubMed: 16373589]
- Young ME, Bray MS. Potential role for peripheral circadian clock dyssynchrony in the pathogenesis of cardiovascular dysfunction. *Sleep Med*. 2007; 8:656–667. [PubMed: 17387040]
- Young ME, Razeghi P, Cedars AM, Guthrie PH, Taegtmeier H. Intrinsic diurnal variations in cardiac metabolism and contractile function. *Circ Res*. 2001; 89:1199–1208. [PubMed: 11739286]
- Zhang Z, He Y, Tuteja D, Xu D, Timofeyev V, Zhang Q, Glatter KA, Xu Y, Shin HS, Low R, Chiamvimonvat N. Functional roles of Cav1.3(alpha1D) calcium channels in atria: insights gained from gene-targeted null mutant mice. *Circulation*. 2005; 112:1936–1944. [PubMed: 16172271]
- Zheng X, Sehgal A. AKT and TOR signaling set the pace of the circadian pacemaker. *Curr Biol*. 2010; 20:1203–1208. [PubMed: 20619819]

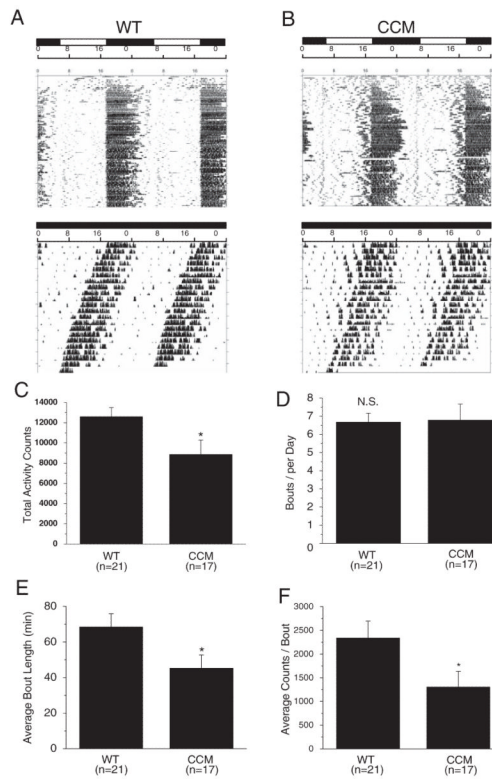
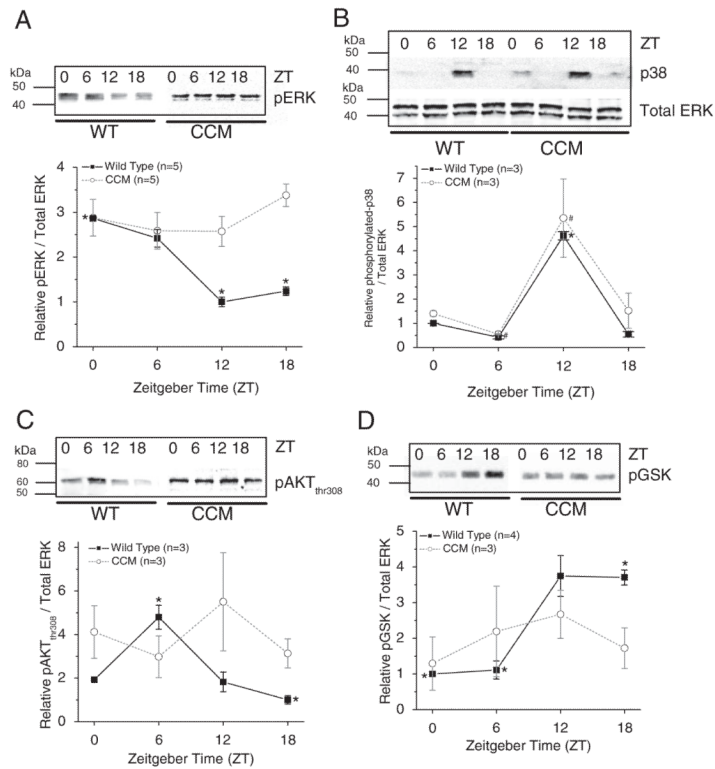


Figure 1.

Wheel-running locomotor activity rhythms in CCM and WT mice. (A and B) Double-plotted wheel-running actograms from a WT mouse (A) housed in LD (top panel) and in DD (lower panel) and from a CCM mouse (B) housed in LD (top panel) and in DD (lower panel). When mice were in LD cycles, the lights were on at 0600 h and off at 1800 h. (C) The WT mice had significantly higher total numbers of wheel revolutions (total activity counts) compared to CCM littermates. (D) There was no difference between WT and CCM mice in total number of bouts per day (bouts per day). (E) The CCM mice had significantly lower length of time for each bout on average (average bout length in minutes) compared to WT mice. (F) The WT mice had significantly higher counts of wheel revolutions for each bout (average counts/bout) compared to CCM mice. WT: $n = 21$; CCM: $n = 17$.

**Figure 2.**

The daily rhythms of protein expression and phosphorylation states in CCM mice and their WT littermates. (A) The phosphorylation of p42/44 ERK was rhythmic in WT mice ($n = 5$), in which diphosphorylated ERK (pERK) peaked at ZT 0. In CCM mice ($n = 5$), pERK was no longer rhythmic. (B) The phosphorylation of p38 kinase was rhythmic in both WT ($n = 3$) and CCM mice ($n = 3$). *Phosphorylated p38 at ZT 12 was significantly higher than ZT 0, 6, and 18 in WT mice. #Phosphorylated p38 at ZT 12 was significantly higher than ZT 6 in CCM mice. (C) The phosphorylation of AKT at thr308 (pAKT_{thr308}) peaked at ZT 6 in WT mice ($n = 3$), while the diurnal rhythm of pAKT_{thr308} was dampened in CCM mouse ($n = 3$) hearts. (D) In WT mouse hearts ($n = 4$), the phosphorylation of GSK3 β (pGSK) was significantly higher at ZT 18 compared to ZT 0 and 6, while there was no diurnal rhythm of pGSK in CCM mice ($n = 3$).

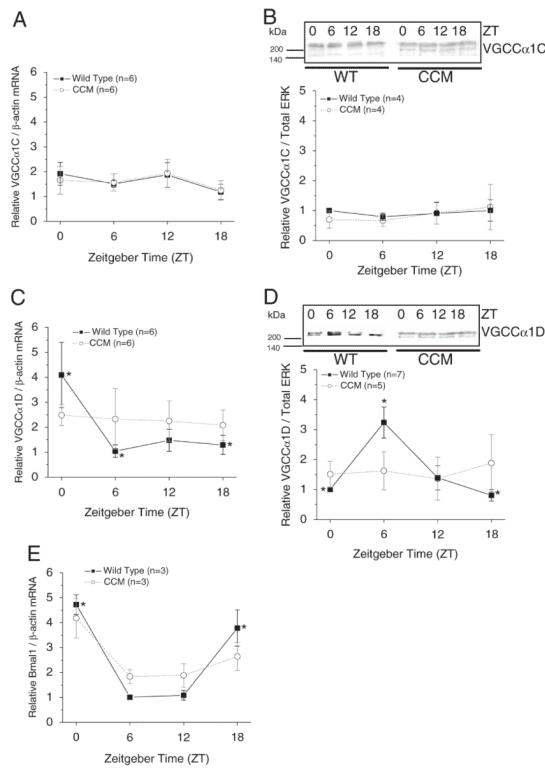


Figure 3.

The daily profiles of *Bmal1*, *VGCCα1C*, and *VGCCα1D* mRNA in CCM mice and their WT littermates. (A) There was no rhythmic expression of *VGCCα1C* mRNA in either WT or CCM mice. $n = 6$ for each time point. (B) The protein expression of *VGCCα1C* was not rhythmic in both WT and CCM mice. (C) The *VGCCα1D* mRNA at ZT 0 was significantly higher than ZT 6 and 18 in WT mice. The diurnal rhythm of *VGCCα1D* mRNA was abolished in CCM mice. $n = 6$ for each time point. (D) In WT mice, the protein expression of *VGCCα1D* peaked at ZT 6, which was significantly different than the protein level at ZT 0 and 18. The diurnal rhythm of *VGCCα1D* was abolished in CCM mice. (E) There was a diurnal rhythm of *Bmal1* mRNA in both WT and CCM mice, but the rhythmic amplitude was smaller in CCM mice. *In WT mice, *Bmal1* levels at ZT 0 and 18 were significantly higher than ZT 6 and 12. $n = 3$ for each time point.